



Journal of Advanced Research in Fluid Mechanics and Thermal Sciences

Journal homepage:
https://semarakilmu.com.my/journals/index.php/fluid_mechanics_thermal_sciences/index
ISSN: 2289-7879



Numerical Exploration of Soret and Dufour Effect on Unsteady Free Convective Radiating Nanofluid Past a Vertical Moving Porous Plate

Aastha^{1,*}, Khem Chand¹

¹ Department of Mathematics & Statistics, Himachal Pradesh University, Shimla, India

ARTICLE INFO

Article history:

Received 16 March 2022
Received in revised form 20 May 2022
Accepted 28 May 2022
Available online 26 June 2022

Keywords:

Radiating; nanofluid; Soret and Dufour effect; moving vertical porous plate; heat and mass transfer characteristics

ABSTRACT

The present paper deals with the numerical investigation of Soret and Dufour effect on free convective heat and mass transfer characteristics of radiating water based nanofluid past a vertically moving porous plate in porous medium. The water based nanofluid with copper as a nanoparticle is considered in the present study. The dimensional governing equations relevant to the present model are transformed into non-dimensional form by using the appropriate parameters. The non-dimensional governing equations with the pertinent boundary conditions are solved numerically by using `bvp4c` function in Matlab software. The influence of suitable parameters on fluid velocity, temperature, concentration, Sherwood number (rate of mass transfer), Nusselt number (rate of heat transfer) and skin friction are exhibited graphically and discussed. Also, the effect of radiation parameter and Prandtl number in the absence of Dufour number has been compared with the help of contours. It is apparent from this study that fluid velocity increases with the increase in K , G_r , G_c & Du and decreases with increase in M^2 . The fluid temperature increases with the increase in Du & R while it decreases with Pr . The fluid concentration increases with increase in S_o whereas it decreases with S_c . The rate of mass transfer (Sherwood number) increases with increase in Du and decreases with increase in S_o & S_c while the rate of heat transfer (Nusselt number) increases with increase in Du & Pr and decreases with increase in R . Shear stress (skin friction) decreases with the increase in G_r , G_c , K & Du .

1. Introduction

The upsurge to the new class generation, known as nanofluids has been there due to the requirement for strengthening the thermal transfer of fluids. Nanofluids have been exhibited to have thermal conductivities superior to large extent than that of liquid alone [1,2]. The word nanofluid is observed to assimilate small nanoparticles having dimensions upto (1-100) nm in the base liquid. The unique physical, chemical and enhanced thermal properties of nanofluids such as thermal conductivity, heat transfer and critical heat flux has enticed the interest of the researchers. Such type of fluids also has high usage in industries because of their higher thermal conductivity in comparison with the other fluids. The recognition of thermic-performance enhancing properties of the nanofluids

* Corresponding author.

E-mail address: aastha2101@gmail.com

<https://doi.org/10.37934/arfmts.97.1.2034>

has added to its applications in various fields such as industrial cooling, nuclear reactors, extraction of geothermal power and other energy sources, cooling of microchips in electronics, as a nanodrug delivery and as a cancer therapeutics in biomedical field. The viscosity model equation hinged on the volume fraction of particles for Al_2O_3 /water nanofluids was brought forward by Maiga *et al.*, [3]. They delineated that when the volume fraction is increased, the effective viscosity also increases for both laminar and turbulent flows. For the (1% - 4%) range of particle volume fraction for the nanoparticle size of 36nm, the variation of temperature in viscosity was formulated by Lundgren [4]. He concluded that for stationary beds Darcy's law with permeability results are concurrent with Brinkmann model results. The thermal analysis of unsteady convective flows over an infinite, vertical, heated, circular cylinder was evaluated by the consideration of generalized Fourier's law of the thermal processes by Shah *et al.*, [5]. The analysis has been carried out with the help of numerical simulations and discussed with the help of graphs. Krishna *et al.*, [6] has analyzed the numerical solution of the unsteady MHD convective rotating flow past an infinite vertically moving porous surface. They analyzed the consequences of thermal radiation and rotation on the surface and the effects of physical variables on fundamental segmentations have been carried out. Turkyilmazoglu and Pop [7] illuminated the heat and mass transfer characteristics of some nanofluid flows past a vertical infinite flat plate and the radiation effect for two distinct types of thermal boundary conditions. They negotiated that the velocity and temperature profiles, skin friction coefficient and Nusselt number inspected may be further utilized for the validation of numerical solutions obtained for more complex transient free convection nanofluid flow problems. The problem of the unsteady MHD free convection flow of nanofluids through a porous medium bounded by a moving vertical semi-infinite permeable flat plate with constant heat source and convective boundary condition in a rotating frame of reference was performed by Das [8]. The effects of different governing parameters on the flow and heat transfer characteristics for two types of nanofluids that is Cu-water and Al_2O_3 -water have been discussed by them. The heat transfer in a porous medium subjected to a magnetohydrodynamic effect and suction velocity adjacent to a vertical plate was evaluated by Ahammad *et al.*, [9]. Their finding was that the thermal gradient at the hot surface reduces with an increased radiation effect.

In a binary mixture, the imposition of a temperature difference enforces the partial separation of the two constituent species. This separation takes place due to the difference in the average molecular velocities of the two species and heavier molecules tend to concentrate to the colder side of the system. It is known as Soret effect. In nanofluids, the Soret effect is demonstrated through the thermophoresis phenomenon. The heat flow due to the isothermal chemical potential gradient is known as the Diffusion thermoeffect or the Dufour effect. The effect of the Dufour phenomenon is in contrast to the effect of a Soret and the creation of thermal flux is due to the chemical potential gradient. The coupled phenomena between the vectorial flows of heat and mass are represented by the Soret and the Dufour effect. For combining the heat and mass transfer problems, there are various formulations and methodologies. Keeping in mind the technological important applications of Soret and Dufour effects in Science and Engineering, these terms have been put in consideration in energy and concentration equations in some recent work. Makinde and Olanrewaju [10] examined an unstable mixed convection with Soret and Dufour effects past a porous plate moving through a binary mixture of chemically reacting fluid. Their conclusion was that the Soret and Dufour effects shouldn't be neglected for the fluids with the medium molecular weight like hydrogen-air mixtures. The numerical investigation of chemical reaction, Soret and Dufour impacts on MHD free convective gyrating flow through a vertical porous channel was conducted by Ahammad and Krishna [11]. It was significantly observed that the Soret impact emerges in suspended mixture of particle and fluids. Quader and Alam [12] presented the numerical solution for Soret and Dufour effects on unsteady

free convection fluid flow in the presence of Hall current and heat flux. The effects of various authorizing parameters have been seen by them. The solution was obtained by using explicit finite difference technique.

Motivated by the above studies, the current study is allocated to numerical investigation of free convective flow of heat-radiating nanofluid through a porous medium past a vertical moving porous plate in a conducting field in the presence of Soret and Dufour effects. The water-based nanofluid having nanoparticles of copper have been considered in this study. The partial differential equations governing the problem along with the corresponding boundary conditions are converted to ordinary differential equations by using Laplace Transform technique and solved by using *bvp4c* function in Matlab software. The effects of various governing parameters involved in the problem are analyzed with the aid of the graphs and discussed in detail.

2. Formulation of the Problem

We consider an unsteady free convective, heat and mass transfer flow of a magneto-nano fluid which is a water-based nanofluid containing nanoparticles of Copper (Cu) past an infinite vertical porous flat plate having an impulsive motion and assimilating Soret and Dufour effects.

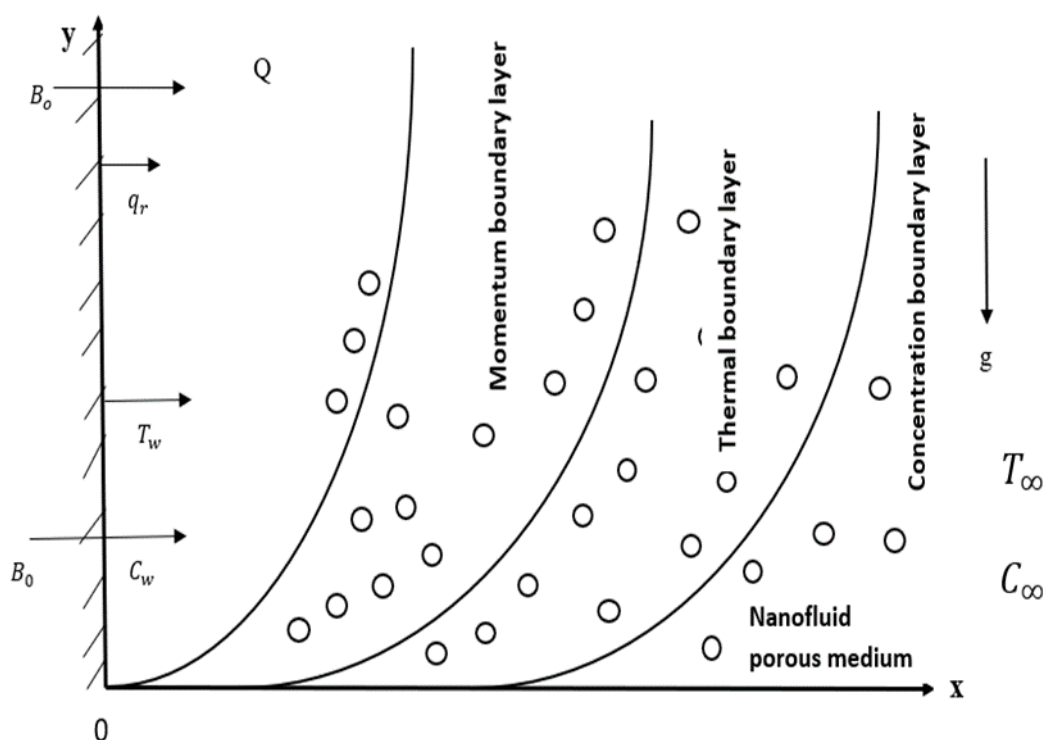


Fig. 1. Geometry of the problem

Here x -axis is taken vertically upwards along the direction of the plate while the y -axis is taken perpendicular to it. A uniform transverse magnetic field B_0 has been applied along the y -axis perpendicular to the plate. Along the plane $Y = 0$, the plate is coincident and for $y > 0$, the flow of the fluid is under restriction. The plate is supposed to be at rest having constant ambient temperature T_∞^* and concentration C_∞^* at time $t = 0$. The plate starts moving in its own plane at time $t > 0$ and having velocity λu_0 vertically with u_0 constant and the temperature of the plate being varied from T^* to T_w^* and the concentration from C^* to C_w^* . Radiative heat flux q_r is also applied in the normal direction to the plate and the mass flux which is caused by the temperature differences and known

as thermal diffusion effect. The base fluid and the nanoparticles which are suspended are in thermal equilibrium. For Cu-water nanofluid, the values related to the thermophysical properties are described. The resulting mixture of Cu-water nanofluid possess a larger thermal conductivity in comparison with the traditional fluids. The existence of the Cu nanoparticles in the water strengthens the effective thermal conductivity of the fluid, it also intensifies the heat transfer characteristics. In the equations of the pattern of the flow of fluid, we suppose that the density has linear dependence on temperature buoyancy forces. We have assumed that the magnetic field $\vec{B} \equiv (0, B_0, 0)$ because of the assumption that in comparison with the applied magnetic field, the induced magnetic field is negligible. Also, there is no external electric field applied so that the polarization of the fluid has a negligible effect and hence we take $\vec{E} \equiv (0,0,0)$. Under the Boussinesq approximation and boundary layer approximation, the conservation equations for momentum, energy and concentration by following Dharmaiah *et al.*, [13] are taken in the form as follows

$$\rho_{nf} \frac{\partial u^*}{\partial t^*} = \mu_{nf} \frac{\partial^2 u^*}{\partial y^{*2}} + g(\rho\beta)_{nf}(T^* - T_\infty^*) + g(\rho\beta^*)_{nf}(C^* - C_\infty^*) - \sigma_{nf} B_0^2 u^* - \frac{\mu_{nf}}{K_p^*} u^* \quad (1)$$

$$(\rho C_p)_{nf} \frac{\partial T^*}{\partial t^*} = k_{nf} \frac{\partial^2 T^*}{\partial y^{*2}} - \frac{\partial q_r^*}{\partial y} (\rho C_p)_{nf} D \frac{\partial^2 C^*}{\partial y^{*2}} \quad (2)$$

$$\frac{\partial C^*}{\partial t^*} = D \frac{\partial^2 C^*}{\partial y^{*2}} + D_1 \frac{\partial^2 T^*}{\partial y^{*2}} \quad (3)$$

$$\mu_{nf} = \frac{\mu_f}{(1 - \phi)^{2.5}}, \rho_{nf} = (1 - \phi)\rho_f + \phi\rho_s,$$

$$(\rho C_p)_{nf} = (1 - \phi)(\rho C_p)_f + \phi(\rho C_p)_s$$

$$(\rho\beta)_{nf} = (1 - \phi)(\rho\beta)_f + \phi(\rho\beta)_s$$

$$(\rho\beta^*)_{nf} = (1 - \phi)(\rho\beta^*)_f + \phi(\rho\beta^*)_s$$

$$\sigma_{nf} = \sigma_f \left[1 + \frac{3(\sigma - 1)}{(\sigma + 2) - (\sigma - 1)\phi} \right], \sigma = \sigma_s / \sigma_f \quad (4)$$

It is prominent that the Eq. (1) to (3) are confined to spherical nanoparticles and have no exposition for the other shapes of the nanoparticles. The effectual thermal conductivity of the nanofluid is as follows

$$k_{nf} = k_f \left[\frac{k_s + 2k_f - 2\phi(k_f - k_s)}{k_s + 2k_f + \phi(k_f - k_s)} \right] \quad (5)$$

The subscripts nf, f and s in Eq. (1) to (5) denotes the thermophysical properties of the nanofluid, base fluid and the nanoparticles respectively. The relevant initial and boundary conditions for the problem are

$$u^* = 0, T^* = T_\infty^*, C = C_\infty^* \text{ for all } y^* \geq 0 \text{ and } t^* = 0$$

$$u^* = \lambda u_0, T^* = T_w^*, C^* = C_w^* \text{ at } y^* = 0 \text{ and } t^* > 0$$

$$u^* \rightarrow 0, T^* \rightarrow T_\infty^*, C^* \rightarrow C_\infty^* \text{ as } y^* \rightarrow \infty \text{ and } t^* > 0 \quad (6)$$

Here λ signifies the direction of the moving plate with $\lambda = 0$, for the plate at the stationary condition and $\lambda = \pm 1$ for the forward and backward motion of the plate. It is presumed that the fluid is an optically thick medium in which the radiation penetration length is small in comparison to the characteristic length. We have used Rosseland approximation for radiative flux for an optically thick fluid. The Rosseland approximation gives the net radiative flux q_r as

$$q_r^* = -\frac{4\sigma^*}{3k^*} \frac{\partial T^4}{\partial y} \quad (7)$$

where $\sigma^* (= 5.67 \times \frac{10^{-8}W}{m^2K^4})$ is the Stefan-Boltzmann constant and $k^*(m^{-1})$ the Rosseland mean absorption coefficient. We assume that the temperature difference within the flow is sufficiently small and the term T^4 may be expressed as a linear function of temperature where T^4 is expanded in Taylor series about a free stream temperature as follow

$$T^4 = T_\infty^4 + 3T_\infty^3(T - T_\infty) + 6T_\infty^2(T - T_\infty)^2 + \dots \dots \quad (8)$$

Neglecting higher order terms in Eq. (8) beyond the first order in $(T - T_\infty)$, we get

$$T^4 \approx 4T_\infty^3T - 3T_\infty^4 \quad (9)$$

Using Eq. (7) and (9), Eq. (2) is written as

$$\frac{\partial T^*}{\partial t^*} = \frac{1}{(\rho C_p)_{nf}} \left(k_{nf} + \frac{16\sigma^* T_\infty^{*3}}{3k_f k^*} \right) \frac{\partial^2 T^*}{\partial y^{*2}} + D \frac{\partial^2 C^*}{\partial y^{*2}} \quad (10)$$

Introducing the following non-dimensional variables

$$y = \frac{u_0 y^*}{v_f}, t = \frac{u_0^2 t^*}{v_f}, u = \frac{u^*}{u_0}, \theta = \frac{T^* - T_\infty^*}{T_w^* - T_\infty^*}, C = \frac{C^* - C_\infty^*}{C_w^* - C_\infty^*}$$

Eq. (1), (3) and (10) takes the following form

$$\frac{\partial u}{\partial t} = \frac{\partial^2 u}{\partial y^2} + Gr A_2 \theta + Gc A_5 C - M^2 A_3 u - \frac{1}{K} u \quad (11)$$

$$\frac{\partial \theta}{\partial t} = \frac{1}{Pr} (1 + R) \frac{\partial^2 \theta}{\partial y^2} + Du \frac{\partial^2 C}{\partial y^2} \quad (12)$$

$$\frac{\partial C}{\partial t} = \frac{1}{S_c} \frac{\partial^2 C}{\partial y^2} + S_o \frac{\partial^2 \theta}{\partial y^2} \quad (13)$$

The prime use of the Laplace Transform Technique is to change an ordinary differential equation in real domain into an algebraic equation in the complex domain, making the equation much easier to solve. By applying Laplace Transform Technique, the Eq. (11) to (13) are transformed into ordinary differential equations as follows

$$\frac{d^2 \bar{u}}{dy^2} - \left(s + M^2 A_3 + \frac{1}{K} \right) \bar{u} + G_r A_2 \bar{\theta} + G_c A_5 \bar{C} = 0 \quad (14)$$

$$\frac{1}{Pr} (1 + R) \frac{d^2 \bar{\theta}}{dy^2} + Du \frac{d^2 \bar{C}}{dy^2} - s \bar{\theta} = 0 \quad (15)$$

$$\frac{1}{S_c} \frac{d^2 \bar{C}}{dy^2} + S_o \frac{d^2 \bar{\theta}}{dy^2} - s \bar{C} = 0 \quad (16)$$

The corresponding initial and boundary conditions for the problem take the following form

$$u = 0, \theta = 0, C = 0 \text{ for all } y \geq 0 \text{ and } t=0$$

$$u = \lambda, \theta = 1, C = 1 \text{ at } y = 0 \text{ and } t > 0$$

$$u \rightarrow 0, \theta \rightarrow 0, C \rightarrow 0 \text{ as } y \rightarrow \infty \text{ and } t > 0 \quad (17)$$

The Eq. (12) to (14) are linear partial differential equations which are to be solved with the initial and boundary conditions (15). It is not possible to find the exact solution for this set of equations, so we solve these equations numerically by using boundary conditions in (17) with the help of `bvp4c` function in Matlab software.

2.1 Some Important Characteristics of Flow Field

2.1.1 Skin friction

In non-dimensional form, the expression for the skin friction is given as

$$\tau = - \left(\frac{du}{dy} \right)_{y=0} \text{ where } \tau = \frac{\tau^1}{\rho U_0^2}$$

2.1.2 Nusselt number

In dimensionless form, the rate of heat transfer in terms of Nusselt number is given as

$$Nu = - \left(\frac{d\theta}{dy} \right)_{y=0}$$

2.1.3 Sherwood number

Also, the rate of mass transfer in terms of Sherwood number in dimensionless form is given as

$$Sh = - \left(\frac{dC}{dy} \right)_{y=0}$$

3. Results and Discussions

To get the outlook of the physics behind the flow regime, the numerical results are interpreted with the help of the graphs. The non-dimensional fluid velocity u , the temperature of the fluid θ and the fluid concentration C have been studied for different values of various parameters such as Schmidt number (S_c), magnetic parameter (M), porosity parameter (K), Grashof number (G_r), modified Grashof number (G_c), Soret number (S_o), Dufour number (Du), Prandtl number (Pr) and Radiation parameter (R).

Also, the variation of Skin friction, rate of heat transfer in terms of Nusselt number (Nu) and rate of mass transfer in terms of Sherwood number (Sh) for different values governing parameters are displayed in the graphs.

3.1 Effect of the Governing Parameters on the Velocity

In Figure 2 to 6, the effect of various governing parameters on the velocity of the fluid has been presented. The solid line in all the figures represents the motion of the plate in the backward direction while the dashed line gives the motion of the plate in the forward direction. In Figure 2, the effect of magnetic parameter (M^2) on the velocity of the fluid is analysed. It is found that the velocity of the fluid shows a decrease with the increasing values of magnetic parameter M for both the moving plate in forward as well as backward direction. This is because in an electrically conducting fluid with the application of a magnetic field, a drag-like force called Lorentz force is produced. So, there is reduction in the velocity of the fluid within the boundary layer because the magnetic field causes an opposition to the transport media. A kind of friction is generated on the velocity of the fluid with the effect of the Lorentz force. Figure 3 depicts the variation in the fluid velocity under the influence of the porosity parameter (K). It is remarked that the velocity of the fluid shows an enhancement with the increasing values of the porosity parameter K for both the motion of plate in backward as well as forward direction. Figure 4 exhibits the effect of Grashof number (G_r) on the velocity of the fluid. The velocity of the fluid u shows an increase with the enhancing values of the Grashof number (G_r) for the moving plate both in backward and forward direction. This is due to the Grashof number acting like a favourable pressure gradient resulting in the acceleration of the fluid within the boundary layer. As a result, the fluid velocity increases with G_r . The Grashof number symbolizes the free convection current effects. Figure 5 reveals the effect of modified Grashof number (G_c) on the velocity of the fluid. It is seen that because of the presence of thermal and solutal buoyancy, there is an increase in the velocity of the fluid with enhancing values of the modified Grashof number (G_c). From Figure 6, the distinction of the velocity of the fluid with respect to Dufour number is elucidated. It is found that the velocity of the fluid increases with the increase in the values of the Dufour number (Du).

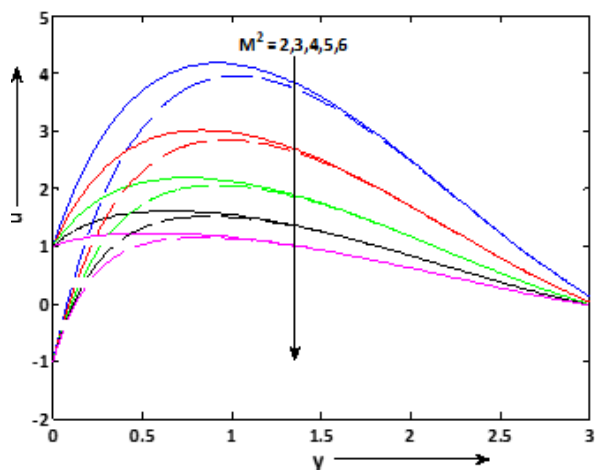


Fig. 2. Effect of M^2 on velocity for $Du = 3, S_o = 5, S_c = 4, K = 1, G_r = 8, G_c = 10, Pr = 0.9, R = 0.5, \lambda = 1$ for solid line & $\lambda = -1$ for dashed line

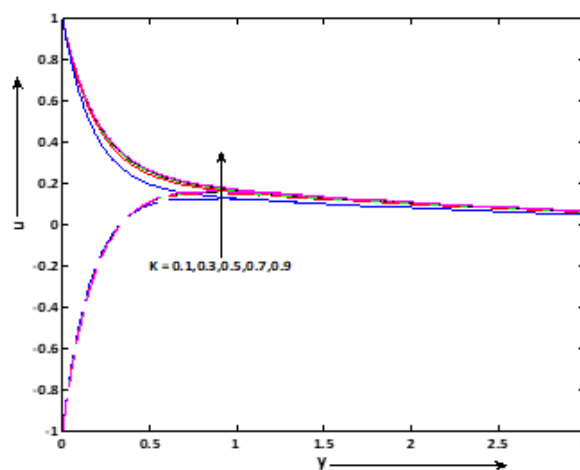


Fig. 3. Effect of K on velocity with $Du = 2, S_o = 2, S_c = 0.22, M^2 = 7, G_r = 2, G_c = 3, Pr = 0.9, R = 0.5, \lambda = 1$ for solid line $\lambda = -1$ for dashed line

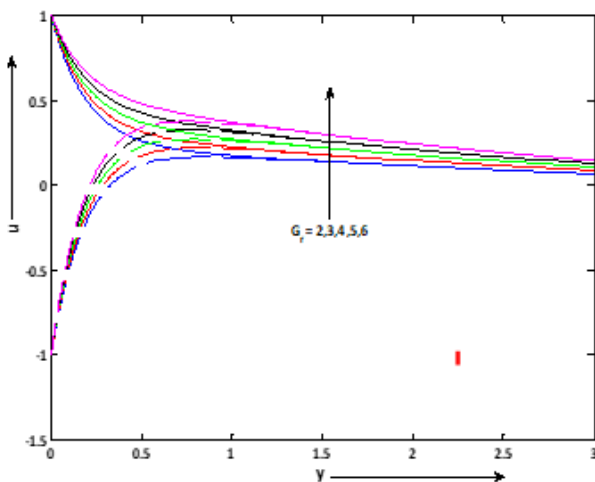


Fig. 4. Effect of G_r on velocity with $Du = 2, S_o = 1, S_c = 0.22, M^2 = 7, K = 0.4, G_c = 3, Pr = 0.9, R = 0.6, \lambda = 1$ for solid line & $\lambda = -1$ for dashed line

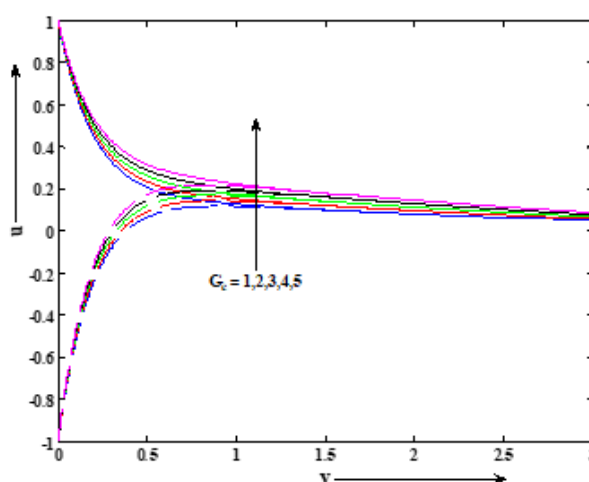


Fig. 5. Effect of G_c on velocity with $Du = 2, S_o = 1, S_c = 0.22, M^2 = 7, K = 0.4, G_r = 2, Pr = 0.9, R = 0.6, \lambda = 1$ for solid line & $\lambda = -1$ for dashed line

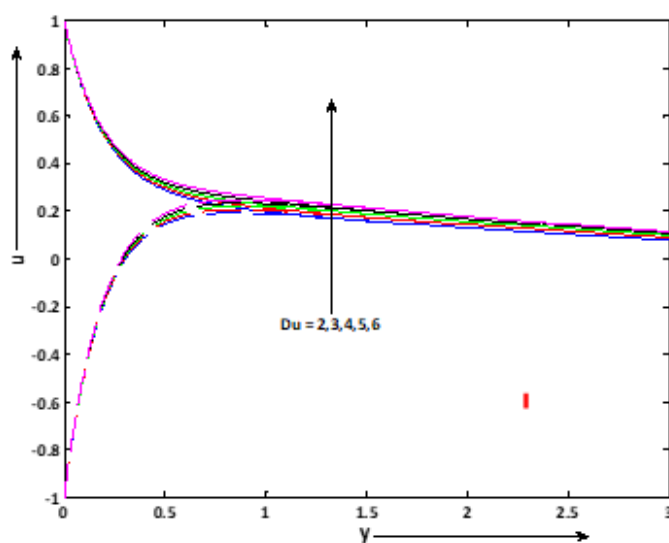


Fig. 6. Effect of Du on velocity with $S_o = 1, S_c = 0.22, M^2 = 7, K = 0.4, G_r = 2, G_c = 4, Pr = 0.9, R = 0.6, \lambda = 1$ for solid line & $\lambda = -1$ for dashed line

3.2 Effect of the Governing Parameters on Temperature

Figure 7 to 9 shows the effect of the various governing parameters on the temperature of the fluid. Figure 7 depicts that the temperature of the fluid elevates with the increasing values of Dufour number (Du). Figure 8 describes that the rise in the values of Prandtl number (Pr) leads to the fall in the temperature of the fluid. Also, the temperature of the fluid increases as the radiation parameter (R) increases which is illustrated in Figure 9. With the increase in the radiation parameter, the heat energy from the flow region is released. There is a decrease in the Rosseland radiation absorption parameter k^* due to decrease in the values of R for given k_{nf} and T_∞ . The rate of radiative heat transfer of the fluid shows a rise because of the increase in the divergence of radiative heat flux leading to the increase in the temperature of the fluid.

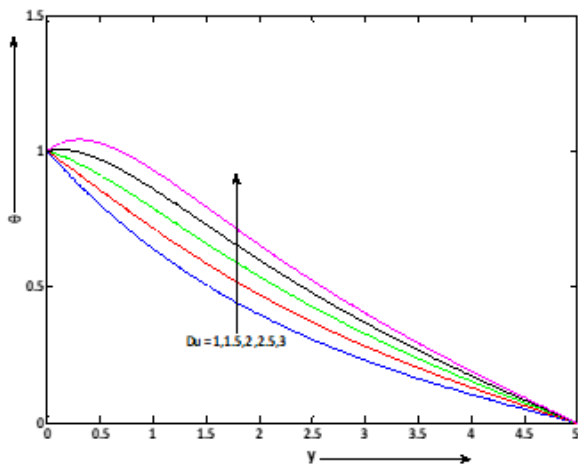


Fig. 7. Effect of Du on temperature with $S_o=1$, $S_c=0.33$, $M^2=9$, $K=0.4$, $G_r=6$, $G_c=6$, $\lambda=1$, $Pr=0.9$ & $R=0.7$

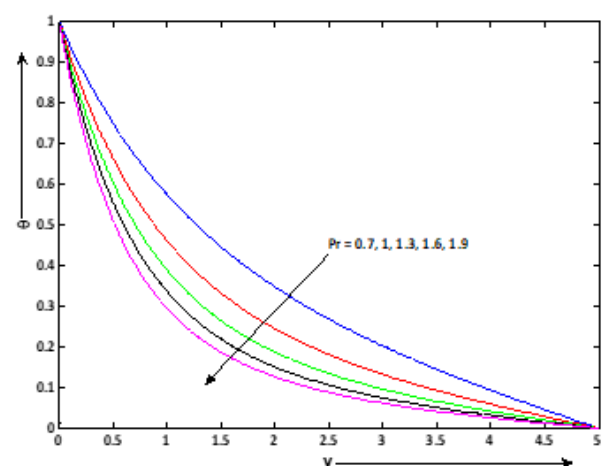


Fig. 8. Effect of Pr on temperature with $Du=1$, $S_o=2$, $S_c=0.27$, $M^2=10$, $K=0.7$, $G_r=4$, $G_c=6$, $\lambda=1$ & $R=0.4$

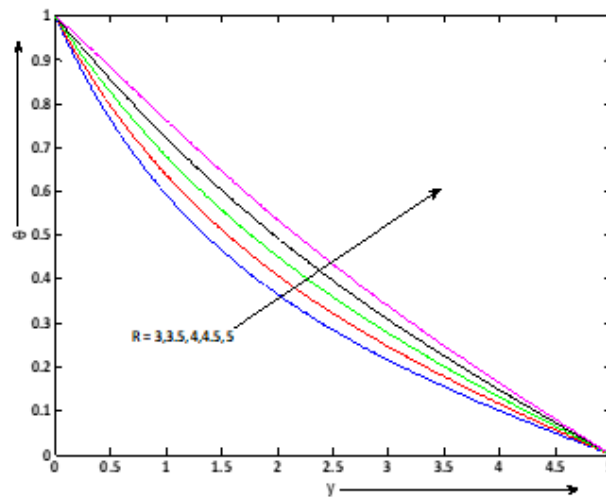


Fig. 9. Effect of R on temperature with $Du=1$, $S_o=3$, $S_c=0.27$, $M^2=10$, $K=0.7$, $G_r=4$, $G_c=4$, $\lambda=1$ & $Pr=1.9$

3.3 Effect of Governing Parameters on Concentration

Figure 10 and 11 represents the effect of various governing parameters on the concentration of the fluid. The Schmidt number symbolizes the ratio of the momentum diffusivity to the species(mass) diffusivity. It is used to characterize fluid flows in which there are simultaneous momentum and mass diffusion convection processes. It physically relates the relative thickness of the hydrodynamic layer and mass transfer boundary layer. Figure 10 illustrates the effect of Schmidt number on fluid concentration. The concentration of the fluid decreases as the value of the Schmidt number (S_c) enlarges while in case of Soret number (S_o) as shown in Figure (11), a reverse effect on fluid concentration is observed with the increasing values of Soret number. The Soret effect recognizes the mass transfer from lower to the higher rate of concentration due to temperature gradient. Therefore, concentration is enhanced due to the increment in the values of the Soret number.

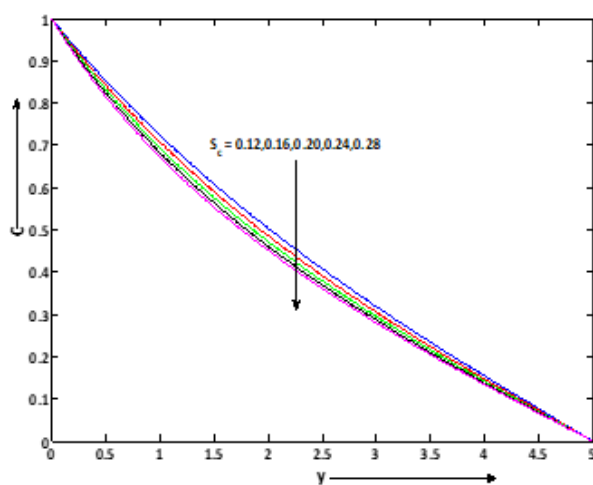


Fig. 10. Effect of S_c on concentration with $Du = 3$, $S_o = 1$, $M^2 = 9$, $K = 0.4$, $G_r = 6$, $G_c = 6$, $\lambda = 1$, $R = 4$ & $Pr = 1.9$

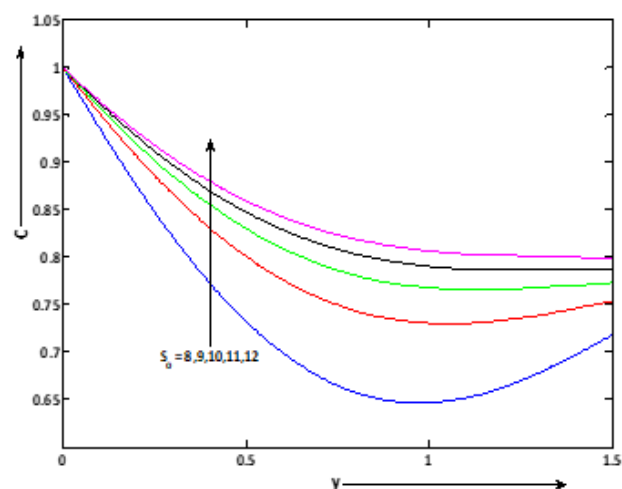


Fig. 11. Effect of S_o on concentration with $Du = 3$, $S_c = 0.44$, $M^2 = 9$, $K = 0.4$, $G_r = 4$, $G_c = 6$, $\lambda = 1$, $Pr = 1.9$ & $R = 4$

3.4 Effect of Governing Parameters on Rate of Mass Transfer at the Plate (Sherwood number)

The non-dimensional rate of mass transfer at the plate $y = 0$ is presented numerically in Figure 12 to 14 for various parameters such as Soret number (S_o), Schmidt number (S_c) and Dufour number (Du). Figure 12 and 13 reveals the variation of Sherwood number with the effect of Soret number (S_o) and Schmidt number (S_c). It is seen that the rate of heat transfer at the plate decreases with the rising values of the Soret number as well as Schmidt number. Figure 14 displays the effect of Sherwood number with respect to the Dufour number showing that the rate of mass transfer rises with the rise in the values of the Dufour number.

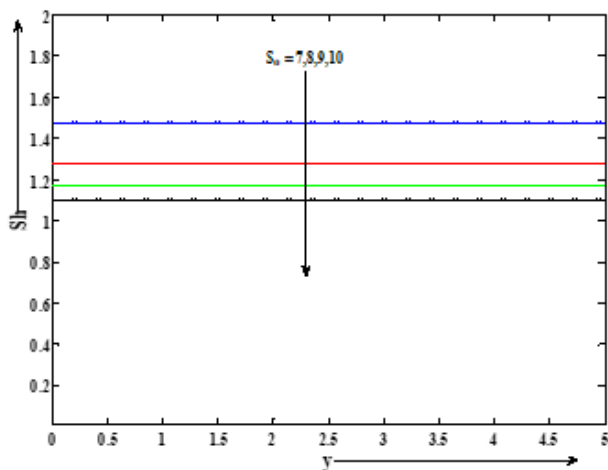


Fig. 12. Effect of S_o on Sherwood number with $Du=2$, $S_c=3.5$, $M^2=3$, $K=0.5$, $G_r=10$, $G_c=12$, $\lambda=1$, $R=0.6$ & $Pr=0.9$

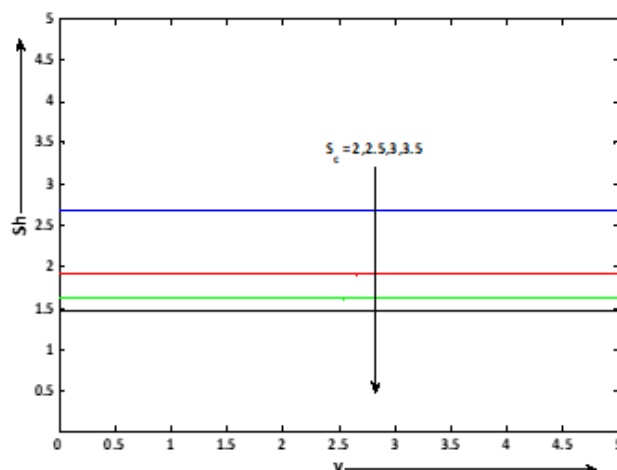


Fig. 13. Effect of S_c on Sherwood number with $Du=2$, $S_o=7$, $M^2=3$, $K=0.5$, $G_r=10$, $G_c=12$, $\lambda=1$, $R=0.6$ & $Pr=0.9$

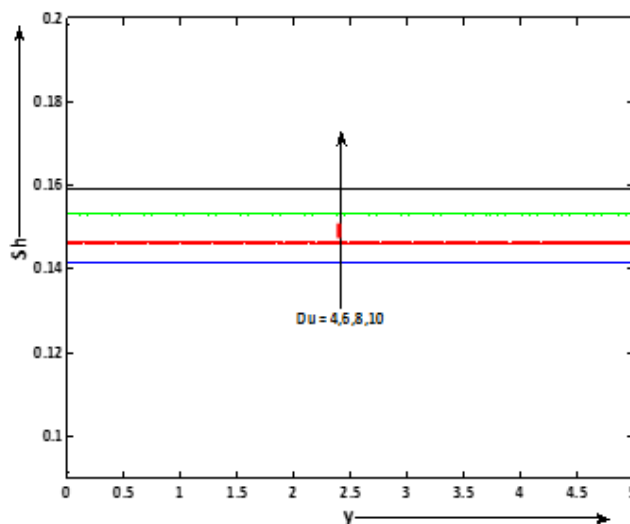


Fig. 14. Effect of Du on Sherwood number with $S_o=7$, $S_c=3.5$, $M^2=3$, $K=9$, $G_r=10$, $G_c=12$, $\lambda=1$, $R=0.6$ & $Pr=0.7$

3.5 Effect of Governing Parameters on the Rate of Heat Transfer at the Plate (Nusselt number)

The values of non-dimensional rate of heat transfer for the motion of the plate in forward direction at $\lambda=1$ is exhibited in Figure 15 to 17 for different values of Dufour number (Du), Radiation parameter (R) and Prandtl number (Pr). As radiation parameter (R) shows an elevation, the rate of heat transfer decreases as is evident from Figure 15 while with the increasing values of Dufour number (Du) and Prandtl number (Pr), a reverse effect is observed as shown in Figure 16 and 17.

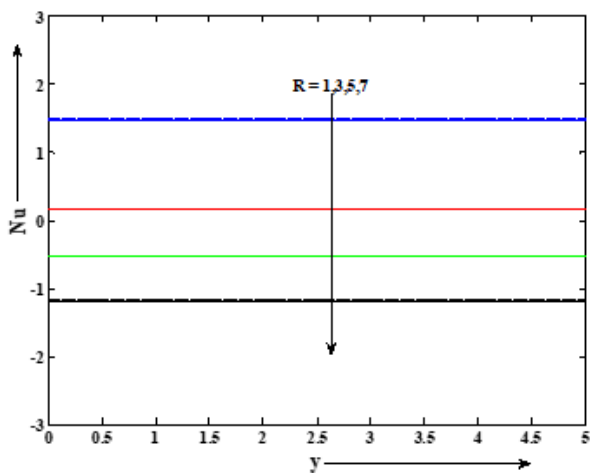


Fig. 15. Effect of R on Nusselt number with $Du = 2$, $S_o = 4$, $S_c = 0.22$, $M^2 = 9$, $K = 0.4$, $G_r = 5$, $G_c = 7$, $\lambda = 1$ & $Pr = 0.9$

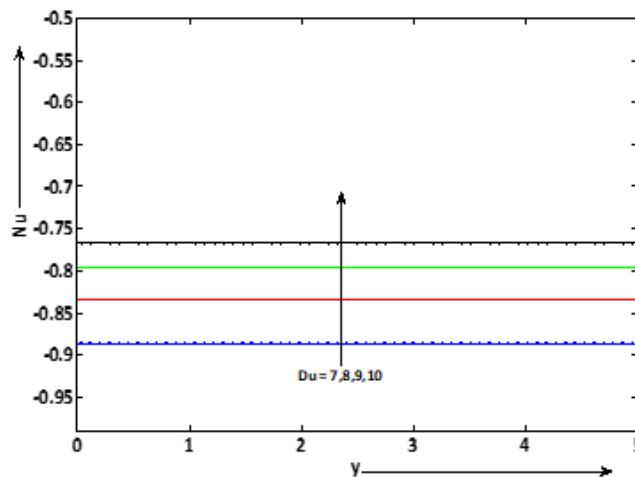


Fig. 16. Effect of Du on Nusselt number with $S_o = 6$, $S_c = 2.5$, $M^2 = 3$, $K = 0.5$, $G_r = 10$, $G_c = 12$, $\lambda = 1$, $R = 0.6$ & $Pr = 0.9$

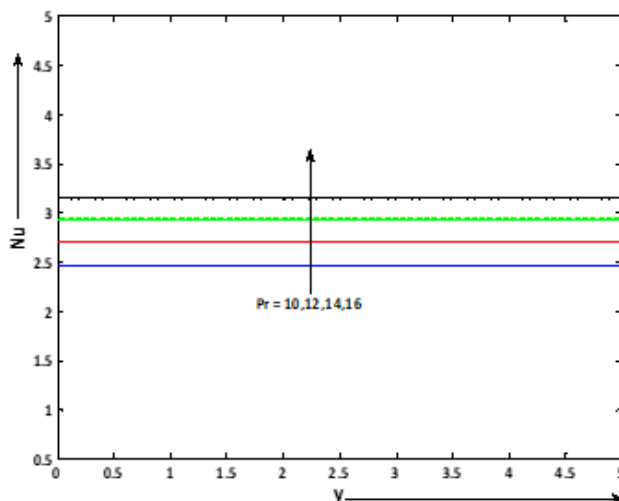


Fig. 17. Effect of Pr on Nusselt number with $Du = 7$, $S_o = 6$, $S_c = 4.5$, $M^2 = 3$, $K = 0.5$, $G_r = 10$, $G_c = 12$, $\lambda = 1$, $R = 0.6$ & $Pr = 0.9$

3.6 Effect of Governing Parameters on Skin Friction (Shear Stress at the Plate)

The non-dimensional skin friction is presented numerically in Figure 18 to 21 under the influence of various parameters such as Grashof number (G_r), modified Grashof number (G_c), porosity parameter (K) and Dufour number (Du). From Figure 18 and 19, it is seen that the skin friction for the plate decreases with the enhancement in the values of Grashof number (G_r) and modified Grashof number (G_c). This is due to the reason that the fluid in the boundary layer undergoes acceleration because of the positive buoyancy forces which act like a favourable pressure gradient, as an outcome, the hot fluid near the plate surface passes away faster as the Grashof number (G_r) increases and so the shear stress at the plate is reduced. The effect of porosity parameter (K) on the shear stress of the plate has been shown in Figure 20. It is observable that the shear stress decreases for decrease in the values of porosity parameter. The influence of Dufour number (Du) on shear stress of the plate is noticed from Figure 21. It is found that the shear stress shows a reduction with the increasing values of the Dufour number.

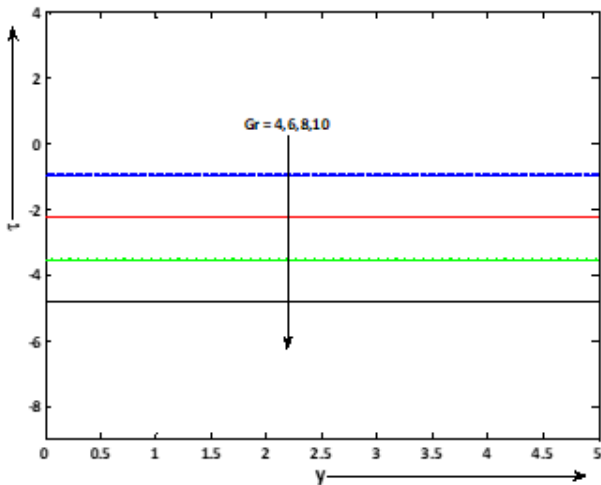


Fig. 18. Effect of G_r on skin friction with $Du = 2$, $S_o = 0.5$, $S_c = 3$, $M^2 = 3$, $K = 0.4$, $G_c = 5$, $R = 7$ & $Pr = 9$

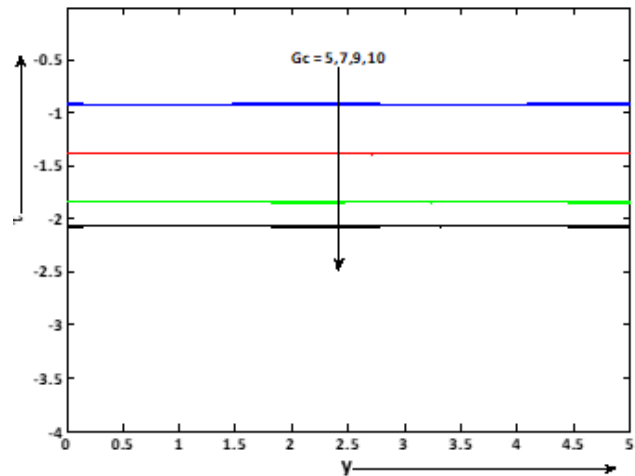


Fig. 19. Effect of G_c on skin friction with $Du = 2$, $S_o = 0.5$, $S_c = 3$, $M^2 = 3$, $K = 0.4$, $G_r = 4$, $R = 7$ & $Pr = 9$

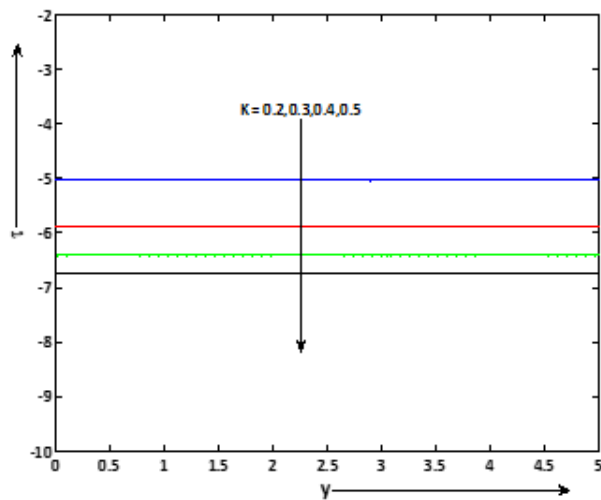


Fig. 20. Effect of K on skin friction with $Du = 2$, $S_c = 2.5$, $M^2 = 3$, $G_r = 10$, $G_c = 12$, $S_o = 6$, $R = 7$ & $Pr = 9$

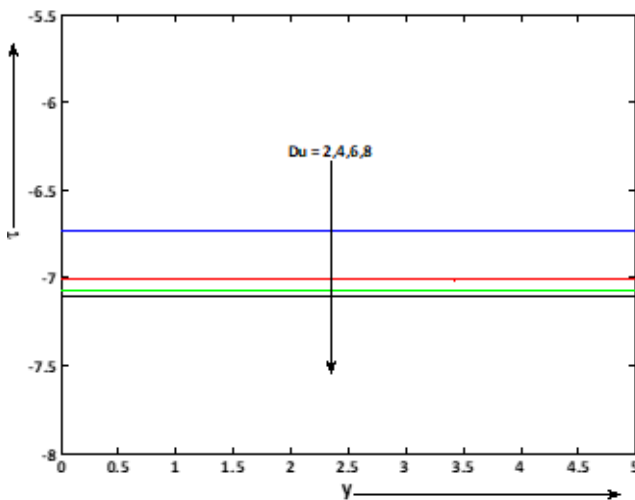


Fig. 21. Effect of Du on skin friction with $S_o = 6$, $S_c = 2.5$, $M^2 = 3$, $K = 0.5$, $G_r = 10$, $G_c = 12$, $R = 7$ & $Pr = 9$

3.7 Comparison of Results

Our study is consistent with the existing study in literature as is evident from the Figure 22 and 23 where our results have been found in conformity with the results obtained by Reddy *et al.*, [14]. The comparative results of the rate of heat transfer with that of the results of Reddy *et al.*, shown by these figures are found to be compatible.

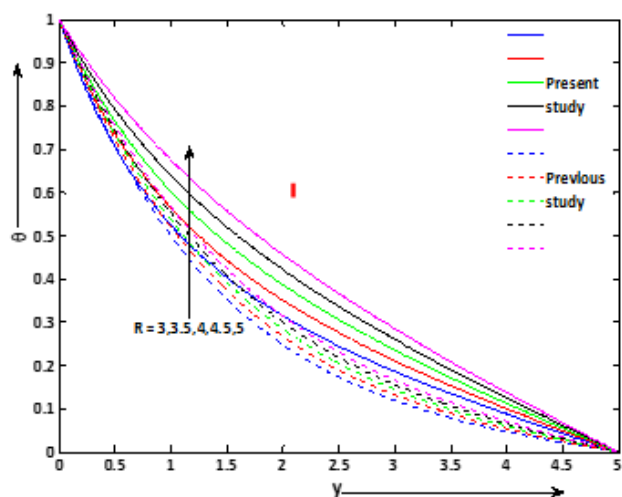


Fig. 22. Comparison of the results. Effect of R on temperature in the absence of Dufour number (Du)

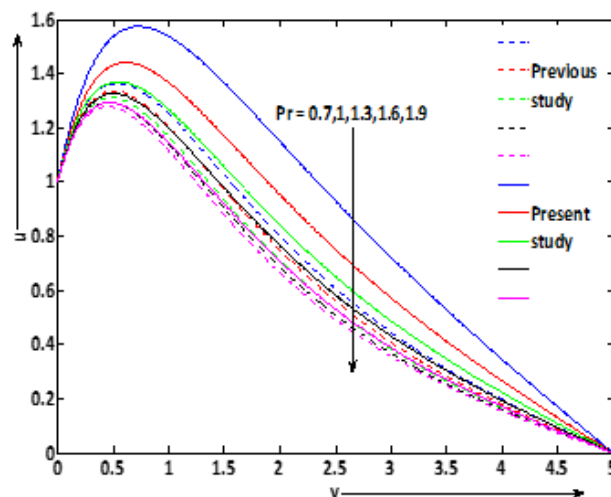


Fig. 23. Comparison of the results. Effect of Pr in the absence of Dufour number (Du)

4. Conclusions

The main aim of present study is to bring out the influence of Soret and Dufour effect on the flow of a radiating Nanofluid past a moving porous plate. The main conclusions of the study is as follows

- i. A rise in the values of porosity parameter (K), Grashof number (G_r), modified Grashof number (G_c) and Dufour number (Du) enhanced fluid velocity whereas reverse effect is observed in case of Magnetic parameter (M^2).
- ii. The temperature of the fluid increases for the increasing values of Dufour number (Du) and Radiation parameter (R) whereas an opposite trend is seen in case of Prandtl number (Pr).
- iii. An increase in Soret number (S_o) results to an enhancement in the concentration of the fluid whereas the study the opposite trend with Schmidt number (S_c).
- iv. The rate of mass transfer (Sherwood number) is intensified with the enlargement in Dufour number (Du) and it decreases for increasing values of Soret number (S_o) and Schmidt number (S_c).
- v. The rate of heat transfer (Nusselt number) rises with the enlarging values of Dufour number (Du) and Prandtl number (Pr) whereas it shows a decline with the increasing value of radiation parameter(R).
- vi. The skin friction i.e., the shear stress reduces for increasing value of Grashof number (G_r), modified Grashof number (G_c), porosity parameter (K) and Dufour number (Du).

Acknowledgement

The authors highly appreciate the valuable comments of the learned referee.

References

- [1] Zhu, Haitao, Canying Zhang, Shiquan Liu, Yaming Tang, and Yansheng Yin. "Effects of nanoparticle clustering and alignment on thermal conductivities of Fe₃O₄ aqueous nanofluids." *Applied Physics Letters* 89, no. 2 (2006): 023123. <https://doi.org/10.1063/1.2221905>
- [2] Hemmat Esfe, Mohammad, Seyfolah Saedodin, Somchai Wongwises, and Davood Toghraie. "An experimental study on the effect of diameter on thermal conductivity and dynamic viscosity of Fe/water nanofluids." *Journal of Thermal Analysis and Calorimetry* 119, no. 3 (2015): 1817-1824. <https://doi.org/10.1007/s10973-014-4328-8>

- [3] Maïga, Sidi El Bécaye, Cong Tam Nguyen, Nicolas Galanis, and Gilles Roy. "Heat transfer behaviours of nanofluids in a uniformly heated tube." *Superlattices and Microstructures* 35, no. 3-6 (2004): 543-557. <https://doi.org/10.1016/j.spmi.2003.09.012>
- [4] Lundgren, To S. "Slow flow through stationary random beds and suspensions of spheres." *Journal of fluid mechanics* 51, no. 2 (1972): 273-299. <https://doi.org/10.1017/S002211207200120X>
- [5] Shah, Nehad Ali, Jae Dong Chung, N. Ameer Ahammad, Dumitru Vieru, and Sadia Younas. "Thermal analysis of unsteady convective flows over a vertical cylinder with time-dependent temperature using the generalized Atangana–Baleanu derivative." *Chinese Journal of Physics* 77 (2022): 1431-1449. <https://doi.org/10.1016/j.cjph.2021.10.013>
- [6] Krishna, M. Veera, N. Ameer Ahammad, and Ali J. Chamkha. "Numerical investigation on unsteady MHD convective rotating flow past an infinite vertical moving porous surface." *Ain Shams Engineering Journal* 12, no. 2 (2021): 2099-2109. <https://doi.org/10.1016/j.asej.2020.10.013>
- [7] Turkyilmazoglu, M., and I. Pop. "Heat and mass transfer of unsteady natural convection flow of some nanofluids past a vertical infinite flat plate with radiation effect." *International Journal of Heat and Mass Transfer* 59 (2013): 167-171. <https://doi.org/10.1016/j.ijheatmasstransfer.2012.12.009>
- [8] Das, Kalidas. "Flow and heat transfer characteristics of nanofluids in a rotating frame." *Alexandria engineering journal* 53, no. 3 (2014): 757-766. <https://doi.org/10.1016/j.aej.2014.04.003>
- [9] Ahammad, N. Ameer, Irfan Anjum Badruddin, Sarfaraz Kamangar, H. M. T. Khaleed, C. Ahamed Saleel, and Teuku Meurah Indra Mahlia. "Heat transfer and entropy in a vertical porous plate subjected to suction velocity and MHD." *Entropy* 23, no. 8 (2021): 1069. <https://doi.org/10.3390/e23081069>
- [10] Makinde, Oluwole Daniel, and Philip Oladapo Olanrewaju. "Unsteady mixed convection with Soret and Dufour effects past a porous plate moving through a binary mixture of chemically reacting fluid." *Chemical Engineering Communications* 198, no. 7 (2011): 920-938. <https://doi.org/10.1080/00986445.2011.545296>
- [11] Ahammad, N. Ameer, and M. Veera Krishna. "Numerical investigation of chemical reaction, Soret and Dufour impacts on MHD free convective gyrating flow through a vertical porous channel." *Case Studies in Thermal Engineering* 28 (2021): 101571. <https://doi.org/10.1016/j.csite.2021.101571>
- [12] Quader, Abdul, and Md Mahmud Alam. "Soret and Dufour Effects on Unsteady Free Convection Fluid Flow in the Presence of Hall Current and Heat Flux." *Journal of Applied Mathematics and Physics* 9, no. 7 (2021): 1611-1638. <https://doi.org/10.4236/jamp.2021.97109>
- [13] Dharmiah, G., N. Vedavathi, K. S. Balamurugan, and J. Prakash. "Heat transfer on mhd nanofluid flow over a semi infinite flat plate embedded in a porous medium with radiation absorption, heat source and diffusion thermo effect." *Frontiers in Heat and Mass Transfer (FHMT)* 9, no. 1 (2017).
- [14] Reddy, P. Chandra, M. C. Raju, and G. S. S. Raju. "Free convective heat and mass transfer flow of heat-generating nanofluid past a vertical moving porous plate in a conducting field." *Special Topics & Reviews in Porous Media: An International Journal* 7, no. 2 (2016). <https://doi.org/10.1615/SpecialTopicsRevPorousMedia.2016016973>
- [15] Das, Sarit K., Stephen U. Choi, Wenhua Yu, and T. Pradeep. *Nanofluids: science and technology*. John Wiley & Sons, 2007. <https://doi.org/10.1002/9780470180693>